Available online at www.sciencedirect.com

ScienceDirect

Procedia IUTAM 10 (2014) 100 – 114

Procedia IUTAM

www.elsevier.com/locate/procedia

23rd International Congress of Theoretical and Applied Mechanics

Multiscale fluid mechanics and modeling

Shiyi Chen[a,*], Moran Wang[b], Zhenhua Xia[a]

[a]*State Key Laboratory for Turbulence and Complex Systems, CAPT, College of Engineering, Peking University, Beijing 100871, China*

[b]*Department of Engineering Mechanics, School of Areospace, Tsinghua University, Beijing 100084, China*

Abstract

In recent years, there has been a tremendous growth of activity on multiscale modeling and computation. In particular, the multiscale hybrid numerical methods are those that combine multiple models defined at fundamentally different length and time scales within the same overall spatial and temporal domain. For examples, a framework of hybrid continuum and molecular dynamics multiscale method has been developed to simulate micro- and nanoscale fluid flows, which combines the continuum computational fluid dynamics (CFD) or the mesoscopic lattice Boltzmann method for the bulk flow region and the atomistic molecular dynamics for the interface region. The similar idea of constrained variation has also been used in developing multiscale fluid turbulent models for constrained dynamic subgrid-scale stress model, Reynolds stress constrained large eddy simulation (RSC-LES) for wall-bounded turbulent flows with massive separation and heat flux constrained large eddy simulation. For RSC-LES, our model is able to solve the traditional log-layer mismatch problem in RANS/LES approaches and can predict mean velocity, turbulent stress and skin friction coefficients more accurate than pure dynamic large eddy models and traditional detached eddy simulation using the same grid resolution. Our results demonstrate the capability of multiscale simulation methods for complex fluid systems and the necessity of physical constraints on the multiscale methods.

Selection and/or peer-review under responsibility of the Organizing Committee of The 23rd International Congress of Theoretical and Applied Mechanics, ICTAM2012

Keywords: fluid mechanics, multiscale modeling, microfluidics and nanofluidics, physical constraints, constrained large eddy simulation

1. Introduction

Multiscale transport phenomena are ubiquitous in fluid dynamic systems, which naturally emerge from the complex interactions among various scales due to the nature of nonlinearity of fluid dynamics. The classical fluid dynamic theories generally care about the fluid only as a continuum which can be

* Corresponding author. Tel.: 86-10-6275-7426; fax: 86-10-6275-7427.
E-mail address: syc@pku.edu.cn.

2210-9838
Selection and/or peer-review under responsibility of the Organizing Committee of The 23rd International Congress of Theoretical and Applied Mechanics, ICTAM2012
doi:10.1016/j.piutam.2014.01.012

described by the Navier–Stokes equations. However as the demands of people's research interests extend, the continuum fluid mechanics may be not sufficient. Figure 1 summarizes theories and typical numerical methods for different temporal and spatial scales. When the continuum assumption breaks down, the fluid has to be described by atomistic point of view, such as the molecular dynamics as a microscopic method or statistical rules for molecular groups, i.e. kinetic theories, as the mesoscopic methods for a larger scale. If the characteristic length is smaller than 1 nm or the characteristic time is shorter than 1 fs, the quantum effect may be not negligible for the concerned system and the quantum mechanics has to be brought in to describe the transport as a result. In fact modeling from a smaller scale may lead to a more accurate description of the problem, but will bring much more computational cost as well. Therefore we may have to find a appropriate tradeoff for our concerned fluid behaviors in engineering.

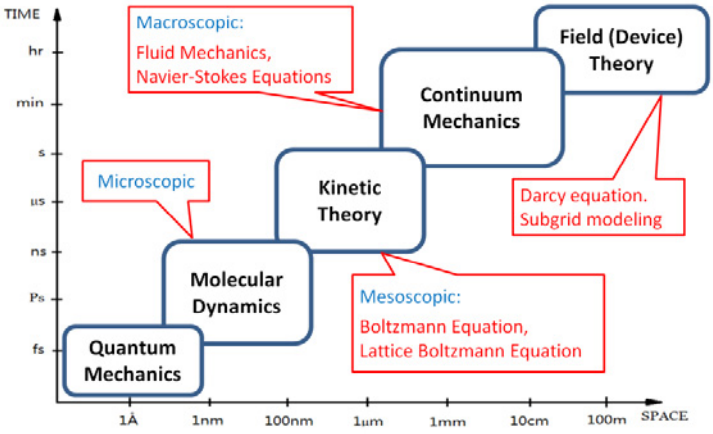

Fig. 1. Theories and methods for different temporal a nd spatial scales.

In spite of significant developments of numerical methods for each scale in recent years, no one single method is capable to satisfy the tremendous demands of revealing physical mechanism and optimizing designs by simulation in fluid flow systems in engineering. Multiscale simulation and modeling has become a necessity. In fact in the past two decades there has been a tremendous growth of activity on multiscale modeling and computation. In particular, the multiscale hybrid numerical methods are those that combine multiple models defined at fundamentally different length and time scales within the same overall spatial and temporal domain. Finding physically consistent solutions in hybrid numerical methods is crucial for various modeling and simulations of fluid mechanics.

Multiscale problems may arise from two aspects: multiscale physical process or hierarchical structure. Therefore we divide the multiscale modeling methods into two categories: the domain decomposition scheme and the averaged equation approach. The domain decomposition scheme corresponds to hybrid continuum molecular models for micro and nanoscale fluid flow, and the averaged equation approach is proposed for multiscale turbulence modeling and simulations. In the following parts of this presentation, we will introduce details of the typical algorithms of each category and demonstrate their capabilities by various applications.

2. Hybrid methods for micro- and nanoscale fluid flow

Micro- and nanoscale fluid flow is a typical case for multiscale modeling where the continuum

assumption may break down somewhere in the flow region. Numerous numerical methods have been developed for simulating or modeling fluid behavior at micro- and nanoscale. Gas flows, for an example, are characterized by the Knudsen number, which is defined as the ratio of the molecular mean free path to a characteristic geometric length or a length over which very large variations of a macroscopic quantity may take place [1], $Kn = \lambda / l$, where λ is the molecular mean free path and l is the characteristic length. Four flow regimes are classified based on the Knudsen number as: continuum flow ($Kn \le 0.001$), slip flow ($0.001 < Kn < 0.1$), transition flow ($0.1 < Kn < 10$), and free molecular flow ($Kn \ge 10$) [2]. The classical computational fluid dynamics (CFD) methods are only valid for the continuum flows. For the slip flow regime, modified boundary conditions including velocity slip and temperature jump are still available to be embedded into CFD methods for engineering approximations. However when the flow falls into the transition flow or free molecular flow regime, the continuum based methods will break down totally. Atomistic simulation methods, including Monte Carlo methods and molecular dynamics (MD) methods, provide an effective way to model fluid flow in these regimes. MD simulations for gas flow are very simple, but the computational efficiency is pretty low. The direct simulation Monte Carlo (DSMC) method, first introduced by Bird [3] for rarefied gas flow, is a relatively more efficient molecular based statistical simulation method for high *Kn* flows, which has been used for modeling of micro gas flows frequently. However, Wang et al. [4] have proved recently that the gas flows in micro and nanoscale are conditionally similar as the rarefied gas flows based on their strict theoretical analysis. If the gas density at micro and nanoscale is high enough to invalidate the perfect gas assumption, DSMC is not available any more. Wang et al. [5] proposed a new Monte Carlo method based on the Enskog theory for dense gas and studied the high density high *Kn* gas flows in micro and nanoscale channels. It is also noticed that the lattice Boltzmann models for microscale gas flows, leaded by Nie et al.[6], have been developed, however the capability of such mesoscopic methods is still limited below the transition flow regime. Even though recently Li and Zhang [7] and Chen et al. [8] have developed unified gas kinetic scheme based on the Boltzmann equation, a full numerical solution of gas flow for the entire flow regimes still depends on coupled multiscale simulations.

When the continuum assumption breaks down in liquid, the best option up to date for modeling is the molecular dynamics simulation. MD has a longer history compared to other atomistic methods and is very simple for simple fluids. The major challenges of algorithm come from the interfacial effects, long range forces or/and multi-field effects. For instance, the electrical or magnetic force is a long range force and has no cut-off unlike the Lenard–Johns force. The main challenge for application lies in the low computational efficiency, which limit its capability to very small spatial region or very short period. Therefore, it has been of great interest and in urgent need to build up a framework of coupling MD at necessary small region with another efficient macroscopic or mesoscopic method at large bulk area smoothly.

Lattice Boltzmann method (LBM) has been a very active mesoscopic numerical tool for fluid flow simulations since late of 1980s [9]. Recently it has been developed to complex flows, including acoustic-fluid interaction [10], electrokinetic flows in complex geometries [11–13], red blood cells or bubble deformations in shear flows [14, 15] and hemodynamics in hierarch vessel systems [16, 17]. More details about latest progress of LBM could be found in the review papers [9, 14]. The advantages of LBM are high efficiency for complex geometry and parallel computing, but the disadvantage comes from its algorithm essence which still always leads to mathematical description consistent with continuum assumption. From this point, LBM is not suitable for finding new fundamental physics in fluid flow, but a great option to be coupled with on the bulk side once the geometry is complex or the physics is complicated (such as with multi-field effects).

As we stated before, no one single method is capable to satisfy the tremendous demands of revealing physical mechanism and optimizing designs by simulation in micro- and nanoscale fluid flow systems. In

this presentation therefore, we introduce a hybrid framework coupling continuum and molecular dynamics methods in which the continuum Navier–Stokes equation or the mesoscopic lattice Boltzmann method is used in the bulk region and the atomistic molecular dynamics at interfaces. We demonstrate its successful capabilities in various fluid problems, including micro-nano fluid flows and heat transfer, singularity problems in the driven cavity, moving contact lines and elcetrowetting and other electrokinetics phenomena. The results prove the feasibility and practicality of multiscale simulation methods for complex fluid systems and the necessity of physical constraints on the multiscale methods.

2.1. Domain decomposition algorithm for simple fluid

Since the continuum only breaks down in a very small region in the flow system, most current multiscale algorithms use the domain decomposition scheme for coupling. Figure 2 shows a general schematic of the geometry of a hybrid scheme. Continuum equations are solved in regions that are homogeneous and have small velocity gradients (shaded region). An atomistic description, for example MD simulation, is used at interfaces or where gradients are large (region with discrete circles). The major technical difficulty in constructing such methods lies in coupling these very different descriptions of fluids at the MD-continuum interface. The two descriptions in the overlap region are coupled and must be consistent, i.e. the physical quantities, including density, momentum and energy, and their fluxes, must be continuous. The boundary conditions needed for the continuum equations can be straightforwardly obtained by averaging the corresponding quantities from the particle description over the local region and over time. However, the reverse problem, generating microscopic particle configurations from known macroscopic quantities such as density, momentum and energy, is non-trivial and must necessarily be non-unique. The problem is magnified when there is flux of particles between continuum and discrete regions. In general, there is also a time coupling issue since the integration time step for the continuum Navier-Stokes equations is normally several orders of magnitude larger than that in the MD region [18].

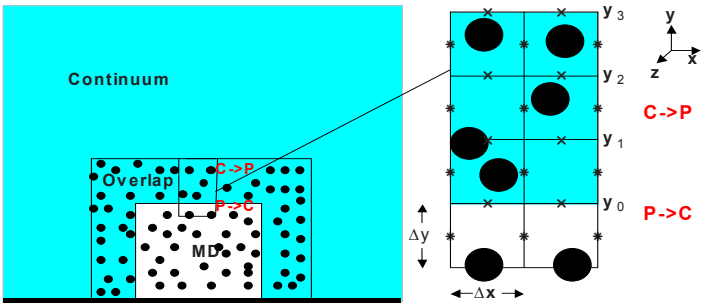

Fig. 2. Illustration of hybrid MD and continuum scheme. The continuum description is used in the shadowed region and the atomistic description is used in the dotted region. In C → P, continuum solutions provide boundary conditions for MD simulations and in P → C atomistic solutions provide boundary conditions for continuum simulations.

Several coupling schemes have been developed, including the relaxation method by O'Connell and Thompson [19], the Maxwell Demon method by Hadjiconstantinou and Patera [20] and so on. In general, the information transfer from MD to continuum is easy by sample-statistics techniques. The major challenge comes from the other side, i.e. information transfer from continuum to MD. The solution is not unique definitely. Here we introduce one method that has been proved effective.

The average continuum velocity u_J in each cell J is obtained by averaging the x-and y-velocities on the

bounding edges. Continuity of the mean velocity requires that the averaged particle velocity in this cell is equal to u_J

$$\frac{1}{N_J}\sum_i \boldsymbol{v}_i = \boldsymbol{u}_J(t), \tag{1}$$

where N_J is the number of particles in cell J. Taking an Lagrangian derivative of the above equation, we have $(1/N_J)\sum_i \ddot{x}_i = \mathrm{D}\boldsymbol{u}_J(t)/\mathrm{D}t$. This constraint requires modification of the usual MD equations of motion: $\ddot{x}_i = F_i/m$, where $F_i = (-\partial/\partial x_i)\sum_{j\neq i} V^{LJ}(r_{ij})$. A general solution of the constraint equation can be written as

$$\ddot{\boldsymbol{x}}_i = \frac{\mathrm{D}\boldsymbol{u}_J(t)}{\mathrm{D}t} + \zeta_i, \tag{2}$$

where ζ_i is a variable whose sum over the cell is constrained: $\sum_i \zeta_i = 0$. To determine the optimum ζ_i we find the extremum of the time integral of the Lagrangian for the particles subject to the non-holonomic constraint of Eq. (1). Following standard derivations we obtain

$$\zeta_i = \frac{\boldsymbol{F}_i}{m} - \frac{1}{N_J m}\sum_{i=1}^{N_J} \boldsymbol{F}_i, \tag{3}$$

which gives the following modified equation for the i-th particle

$$\ddot{\boldsymbol{x}}_i = \frac{\boldsymbol{F}_i}{m} - \frac{1}{N_J m}\sum_{i=1}^{N_J} \boldsymbol{F}_i + \frac{\mathrm{D}\boldsymbol{u}_J(t)}{\mathrm{D}t}. \tag{4}$$

To prevent molecules from freely drifting away from the MD simulation domain, an external force is applied to particles between y_2 and y_3 (as shown in Fig. 2)

$$F_y = -\alpha p_0 \sigma \frac{(y - y_2)}{1 - (y - y_2)/(y_3 - y_2)}. \tag{5}$$

Here p_0 is the average pressure in the MD region, and α is a constant of order one. In our work we use $y_3 - y_2 = \Delta y$ and $\alpha = 1$, but the hybrid solution is not sensitive to factor of 2 changes in either parameter. The key constraints are that F_y confine particles while minimizing density oscillations.

After validations, the proposed multiscale method has been used to simulate a microchannel flow with nanoscale rough walls, which has many application backgrounds in MEMS and Lab-on-Chip devices. Figure 3a shows the schematic of physical model of channel flow with nanoscale roughness on bottom wall abstracted from engineering applications. We are caring about how the nanoscale roughness influences the bulk flow in channel. Figure 3b shows the streamlines around one roughness from the hybrid modeling compared with full MD simulations or with pure continuum simulation. The results indicate that the hybrid method agrees quite well with the full MD simulation but deviates clearly from the pure continuum modeling, which also suggests that the continuum description on this problem, consisting of the NS equations and non-slip boundary conditions, does not capture the relevant physics and the hybrid modeling is necessary indeed. Furthermore, this method has been developed for heat transfer problem in channel flows [21], singularity problems in upper-driven cavity flows [22], moving contact lines, and time multiscale coupling problems [23].

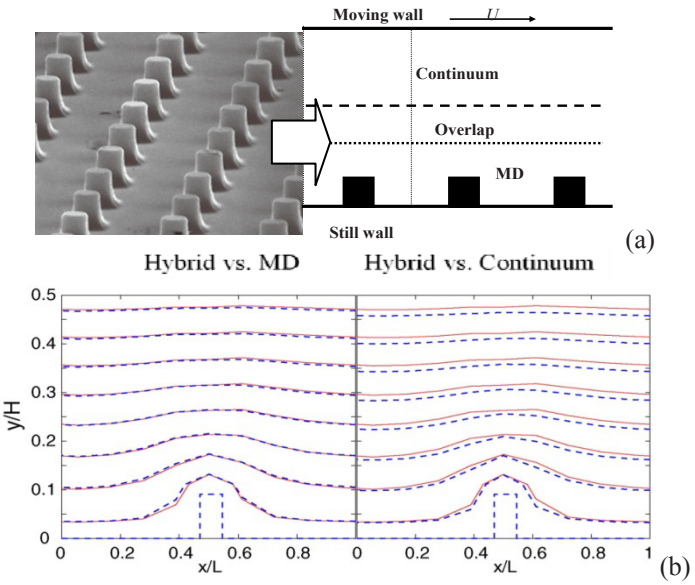

Fig. 3. Multiscale modeling of channel flow with nanoscale roughness on bottom wall. (a) Physical model abstracted from engineering application; (b) streamlines comparisons around one roughness: the solid lines are from the hybrid modeling, the dashed line on the left is from the full MD simulation and dashed line on the right is from the full continuum modeling (CFD).

2.2. Hybrid algorithm for electrokinetic fluid

In micro- and nanoscale fluid flow, the surface forces play more important roles than body forces. Especially, the electrical force is very popular in liquid flows for polar-molecule liquid, such as water. Even though without any extra ions, the solid surface will also be charged by chemical adsorption or dissociation of solid molecular groups at the solid-liquid interface [24, 25]. Therefore to reveal transport mechanisms of electrokinetic fluid at micro- and nanoscale is of great interests and in urgent demand. The major challenge of MD simulations for electrokinetic fluid comes from the long-range Coulomb force. Since there is no cut-off like the LJ potential, a full MD modeling of electrokinetic fluid with direct summation of electrical force between each ion will cost extremely high computational resources. A few methods have been proposed, such as particle-mesh-Ewald (PME) [26], and fast-multipole method (FMM) [27]. Here we introduce a hybrid algorithm, particle-particle particle-mesh method (P^3M), inspired by the many-body treatments in the astrophysical field, which really embody the idea of multiscale solution [28].

A two-dimensional schematic of the P^3M is displayed in Fig. 4. In this method, we divide the total force of the concerned particle into two parts: short-range force within a distance, such as in the cycle in Fig. 4, and long-range force outside the distance. The short-range interactions from both Coulomb and van der Waals forces are treated precisely with the Particle-Particle (PP) method by direct summation; while the long-range interactions are calculated with the Particle-Mesh (PM) method by solving a Poisson equation for electrical potential on a mesh. Both the advantages of the accuracy of the PP method and the efficiency of the PM method can be achieved through this approach. The details about this hybrid algorithm can be found in our recent paper [29]. We used a high-efficiency multi-grid method to solve the Poisson equation in each time step so as to lower its computational cost scale as $O(N_G)$.

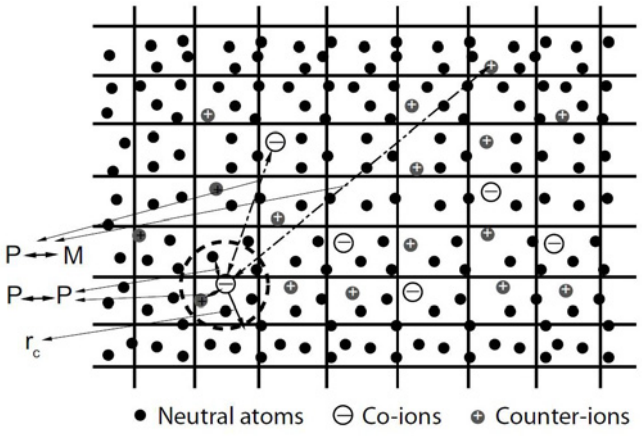

Fig. 4. A two-dimensional schematic of the P^3M algorithm. The simulations are actually three-dimensional. Lines indicate the mesh which has spacing h_x and h_y along horizontal and vertical directions. Short-range contributions (P↔P) are obtained by direct summation over nearby particles with a radius r_c (dashed circle). Long range contributions (P↔M) are obtained from the particle-mesh method.

Using this hybrid method, we studied electroosmotic flow in nanochannels with regular or random roughness on the walls. The results show that roughness reduces the electroosmotic flow rate dramatically even though the roughness is very small compared to the channel width. Systematic investigation of the effect of surface charge density and random roughness will help to better understand the mechanism of electrokinetic transport in rough nanochannels and to design and optimize nanofluidic devices.

Another important and interesting application of this hybrid modeling method is to reveal mechanism of electrowetting. As well known electrowetting has numerous applications in Lab-on-a-chip, microlenses, display control and soft printing etc. The contact angle variation with the applied electric voltage can be described by the Young–Lippmann's equation (YLE). Experiments have observed electrowetting with a wide range of fluids and substrates. In all cases, results follow the YLE at small V but saturate before perfect wetting is achieved. A variety of mechanisms have been proposed, but no consensus has emerged for its origin yet. Therefore we tried to reveal its inherent mechanism by simulations because simulations can provide some essential details which are not measurable by experiments.

Figure 5a–5c graphically demonstrates how θ varies with V and how θ is measured. Figure 5d shows $\theta(V)$ for a wide range of parameters. In each case, the results follow YLE at low V and then saturate. These results provide strong evidence that the YLE remains valid down to nanometer scales. Figure 5e shows the peak electric force on molecules at the interface for a range of systems. The linear rise depends on the factors that determine $\theta(V)$ but is independent of chain length. In the simulations, saturation occurs when ions are pulled from the drop by large local fields. Saturation can be controlled by changing temperature, screening, or the energy binding ions to the fluid. We show a local force balance equation for θ remains valid even after saturation and that the interface approaches the equilibrium contact angle within a few nanometers of the solid [30].

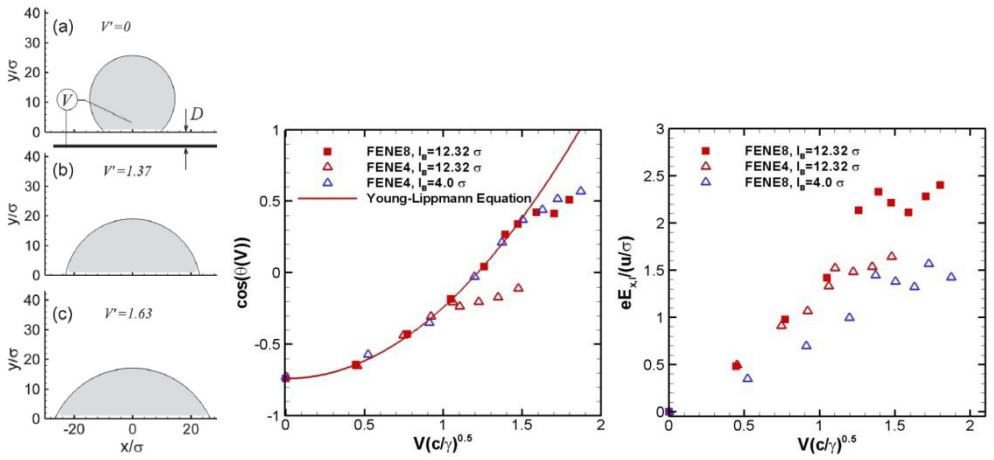

(d) (e)

Fig. 5. (a)–(c) As the dimensionless voltage $V' \equiv V(c/\gamma)^{0.5}$ between a cylindrical drop and electrode (thick line) increases, the drop (shaded area) spreads along a dielectric of thickness $D = 4.86\sigma$. Solid lines show cylindrical fits to the drop surface for $y > 6\sigma$. (d) Change in contact angle θ with dimensionless voltage and prediction by Young–Lippmann equation; (e) Variation of the electric force at the interface, $e\boldsymbol{E}_{x,i}$, with V for $\theta_0 = 138°$. Squares and triangles are for chains with 8 and 4 beads, respectively.

3. Multiscale modeling in turbulence simulation: constrained large-eddy simulation

As is already known to the community, turbulence is a complex flow which consists of a continuous spectrum of scales, both spatial and temporal, ranging from the largest to the smallest. In industrial applications, including the stalled wing, fuselages at high incidence, turbine blades and vehicle bodies, the flows are always turbulence with massive separations. For these kinds of complex turbulent flows, it is very important to accurately predict the separation and reattachment characteristics. In general, there are three types of turbulence simulation methods, including direct numerical simulation (DNS), large eddy simulation (LES) and Reynolds-averaged Navier–Stokes (RANS). DNS solves the Navier–Stokes equations directly with certain boundary and initial conditions, resolving all the scales of motions. It is the simplest approaches conceptually. However, it is limited by the numerical requirements and computational cost, and not applicable for industry flows. RANS is the mostly used engineering method in current days. It solves the mean velocity equations with RANS models. It works pretty well in most attached turbulent flows. However, it usually cannot accurately predict non-equilibrium and unsteady flows with separations. In LES, the larger scale turbulent motions are directly solved, whereas the effects of the smaller-scale motions are modeled. It can be used to simulate the unsteady flows. In general, its computational cost is much less than DNS. However, when it is used in wall-bounded turbulent flows, the cost increases a lot which impedes the applications of LES in industry flows.

3.1. Hybrid RANS-LES method

Among all, hybrid RANS-LES method, including the detached eddy simulation method (DES), is the most popular approach for complex wall-bounded turbulent flows at high Reynolds numbers. In hybrid method, RANS is used in the near wall region to avoid huge grid resolution demand for LES, while LES is used for the outer region. The two solutions are matched with each other at certain locations. The hybrid RANS-LES method has achieved great success in engineering applications [31–33]. However, it suffers from the discrepancy of the log-law intercepts between numerical results and experiments in

simple turbulent channel flows (the so-called log-layer mismatch, LLM) [31–34]. This defect casts doubts on the results obtained by such approaches, especially for the problems where the near-wall flow plays an important role. Please see the review papers by Fröhlich and von Terzi [33] and Spalart [32] for more details on hybrid RANS-LES method.

The physical origin of LLM in hybrid RANS-LES method stems from the methodology itself. In the RANS region, especially in the attached ones, the flow is smooth with laminar-like long unphysical streaks. In this region, the flow is diffusion dominated. On the other hand, the flow is turbulent with abundant fluctuations in the LES region, which is convection dominated. When the two results are matched together, the lack of small scale fluctuations in the RANS area becomes the mains shortcoming, resulting in the underestimated Reynolds stresses in the transition region and then LLM. To find a natural solution to the RANS-LES transition problem is an important step toward the overall success of the hybrid RANS-LES methods.

3.2. Constrained large eddy simulation for isotropic turbulence flows

In LES, the most critical issue is the subgrid-scale model rising from the nonlinear term in the Navier-Stokes equations. Since the constrained decimation theory first proposed by Kraichnan [35], researchers have tried to apply physical constraints on the SGS turbulence model. In constrained decimation theory, Kraichnan separated the Fourier modes into inner modes (retained scales, large scales) and outer modes (residual scale, subgrid scales, SGS). He solved mode-reduced retained motions, while the effect of the residual scales on the retained scales is modelled by a stochastic forcing. In order to correctly calculate the mean energy flux, the forcing term is constrained to satisfy certain constraint equations deduced from underlying physics, such as symmetry and conservation. Kraichnan and Chen [36] extended the decimation idea to study intermittent phenomena in fluid turbulence by enforcing more constraints on high order statistics. A recent success in isotropic turbulence is the constrained dynamics SGS (C-SGS) model proposed by Shi et al. [37]. In their model, they implemented an energy dissipation constraint on the traditional dynamic SGS model as follows

$$\left\langle T_{ij}^{\mathrm{mod}}\,\overline{\tilde{S}}_{ij}\right\rangle = \left\langle \left(L_{ij}+\overline{\tau_{ij}^{\mathrm{mod}}}\right)\overline{\tilde{S}}_{ij}\right\rangle \ . \tag{6}$$

Here, a tilde denotes filter at grid scale Δ, an overbar represents a test filter at scale 2Δ. τ_{ij}^{mod} and T_{ij}^{mod} are the modelled SGS stress at scale Δ and 2Δ, $L_{ij}=\overline{\tilde{u}_i\tilde{u}_j}-\overline{\tilde{u}}_i\overline{\tilde{u}}_j$ is the resolved stress tensor, $\overline{\tilde{S}}_{ij}$ is the strain rate tensor at scale 2Δ.

They verified the C-SGS model in statistically steady and freely decaying isotropic turbulence flows. The results were compared with those obtained from the non-constrained mixed SGS model and DNS, showing that the constrained SGS (C-SGS) model not only predicts the turbulent dissipation accurately, but also shows a strong correlation with the real stresses from a priori test. As the physical space decimation constraint, the C-SGS models improve other features of the dynamic mixed model, including ability to predict the probability density distribution of the SGS stress and the energy backscatter (see Fig. 6).

3.3. Constrained large eddy simulation for wall-bounded turbulence flows

Encouraged by the above successes of the physical constraint idea in turbulence modeling, Chen et al. [38] proposed a new methodology, called constrained large eddy simulations (CLES), for simulating high Reynolds number wall-bounded turbulent flows, both attached and detached. Different from hybrid RANS-LES methods, large eddy simulation is carried out across the whole domain in CLES method,

while enforcing a Reynolds-stress constraint on the SGS model in the inner layer region to ensure that a prescribed Reynolds-stress condition is satisfied. The underlying physics of constraining the Reynolds stresses is based on the belief that the Reynolds stresses are the most important quantities that control the mean flow dynamics for the LES of wall-bounded turbulent flows.

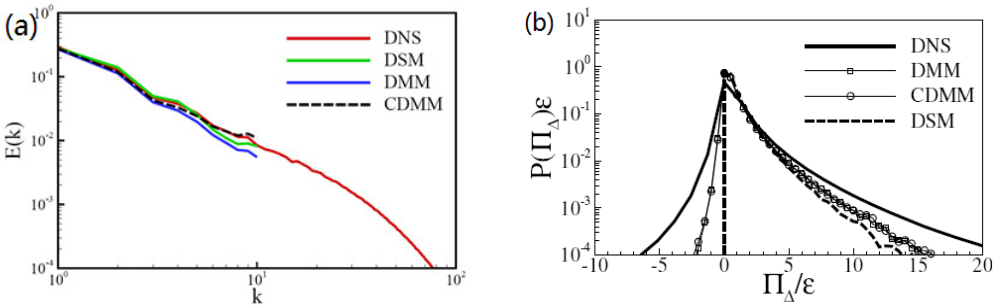

Fig. 6. (a) Comparison of energy spectrum of steady isotropic turbulence for *a posteriori*. Red solid line: DNS; green solid line: Dynamic Smagorinsky model, DSM; blue solid line: Dynamic mixed similarity model, DMM; black dashed line: constrained dynamic mixed model, CDMM. (b) Comparison of probability density functions for the energy flux at grid scales for *a posteriori*. Bold solid line: true flux from DNS; line with squares: DMM; line with circles: CDMM; dashed line: DSM [37].

Considering LES of incompressible turbulence flows, the following low-pass filtered Navier–Stokes equations for large scales are solved

$$\frac{\partial \tilde{u}_i}{\partial x_i} = 0, \tag{7}$$

$$\frac{\partial \tilde{u}_i}{\partial t} + \frac{\partial \tilde{u}_i \tilde{u}_j}{\partial x_j} = -\frac{\partial \tilde{p}}{\partial x_i} + \nu \frac{\partial^2 \tilde{u}_i}{\partial x_j \partial x_j} - \frac{\partial \tau_{ij}}{\partial x_j}. \tag{8}$$

Here, a tilde denotes low-pass filtering, $\tilde{u}_i$ is the large-scale velocity, $\tilde{p}$ is the filtered pressure, ν is the kinetic viscosity and τ_{ij} is the SGS stresses

$$\tau_{ij} = \widetilde{u_i u_j} - \tilde{u}_i \tilde{u}_j \ . \tag{9}$$

When we perform the ensemble average operator $\langle \cdot \rangle$ on Eq. (8), we obtained the following equation for the mean large scale velocity

$$\frac{\partial \langle \tilde{u}_i \rangle}{\partial t} + \frac{\partial \langle \tilde{u}_i \rangle \langle \tilde{u}_j \rangle}{\partial x_j} = -\frac{\partial \langle \tilde{p} \rangle}{\partial x_i} + \nu \frac{\partial^2 \langle \tilde{u}_i \rangle}{\partial x_j \partial x_j} - \frac{\partial \langle \tau_{ij} \rangle}{\partial x_j} - \frac{\partial R_{ij}^{LES}}{\partial x_j} \ . \tag{10}$$

Here,

$$R_{ij}^{\mathrm{LES}} = \langle \tilde{u}_i \tilde{u}_j \rangle - \langle \tilde{u}_i \rangle \langle \tilde{u}_j \rangle \ . \tag{11}$$

is called the resolved Reynolds stress. If one compares Eq. (10) with the Reynolds-averaged Navier–Stokes equations [39] and assumes that the flow is ergodic, the following expression for Reynolds stress $R_{ij}^{\mathrm{LES}} = \langle \tilde{u}_i \tilde{u}_j \rangle - \langle \tilde{u}_i \rangle \langle \tilde{u}_j \rangle$ holds

$$R_{ij}^{\mathrm{RANS}} = R_{ij}^{\mathrm{LES}} + \left\langle \tau_{ij} \right\rangle . \tag{12}$$

From the above equation, we can easy obtain the mean of τ_{ij} as follows, so long as R_{ij}^{RANS} is known or estimated by some RANS model

$$\left\langle \tau_{ij}^{\mathrm{SGS}} \right\rangle = R_{ij}^{\mathrm{RANS}} - R_{ij}^{\mathrm{LES}} . \tag{13}$$

So we can estimate the τ_{ij} in the inner layer from two parts

$$\tau_{ij}^{\mathrm{SGS}} = \left\langle \tau_{ij}^{\mathrm{SGS}} \right\rangle + \tau_{ij}' \ . \tag{14}$$

The first part is the mean part, which is constrained by the Eq. (13); the second part is the fluctuating part. They proposed a very simple form based on the Smagorinsky model to model this part

$$\tau_{ij}' = -2C_S' \left(\left|\overline{\Delta}\right|^2 \left|\tilde{S}\right| \tilde{S}_{ij} - \left\langle \left|\overline{\Delta}\right|^2 \left|\tilde{S}\right| \tilde{S}_{ij} \right\rangle \right) , \tag{15}$$

where the coefficient C_S' can be estimated using the standard dynamic procedure. So the final constrained SGS model in the inner layer is as follows

$$\tau_{ij}^{\mathrm{SGS}} = R_{ij}^{\mathrm{RANS}} - R_{ij}^{\mathrm{LES}} - 2C_S' \left(\left|\overline{\Delta}\right|^2 \left|\tilde{S}\right| \tilde{S}_{ij} - \left\langle \left|\overline{\Delta}\right|^2 \left|\tilde{S}\right| \tilde{S}_{ij} \right\rangle \right), \tag{16}$$

Jiang et al. [40] followed the physical constraint idea and extended it to compressible wall-bounded turbulent flows. As there is one more governing equation for the energy, they introduced three more constraints for the subgrid-scale heat fluxes, besides the Reynolds stress constraints for the momentum equations. The constrained subgrid scale model for the SGS stresses and heat fluxes are

$$\begin{aligned} \tau_{ij}^{\mathrm{SGS}} &= R_{ij}^{\mathrm{RANS}} - \left(\left\langle \overline{\rho}\tilde{u}_i\tilde{u}_j \right\rangle - \left\langle \overline{\rho}\tilde{u}_i \right\rangle \left\langle \overline{\rho}\tilde{u}_j \right\rangle / \left\langle \overline{\rho} \right\rangle \right) \\ &\quad - 2C_s' \left[\overline{\rho} \left|\overline{\Delta}\right|^2 \left|\tilde{S}\right| \left(\tilde{S}_{ij} - \frac{1}{3}\tilde{S}_{kk}\delta_{ij} \right) - \left\langle \overline{\rho} \left|\overline{\Delta}\right|^2 \left|\tilde{S}\right| \left(\tilde{S}_{ij} - \frac{1}{3}\tilde{S}_{kk}\delta_{ij} \right) \right\rangle \right], \end{aligned} \tag{17}$$

$$\begin{aligned} Q_j^{\mathrm{SGS}} &= \left\langle \tilde{u}_j(\overline{\rho}\tilde{e} + \overline{p}) \right\rangle - \left\langle J_j^{\mathrm{LES}} \right\rangle - \left(\left\langle \overline{\rho}\tilde{e} \right\rangle + \left\langle p \right\rangle \right) \left\langle \overline{\rho}\tilde{u}_j \right\rangle / \left\langle \overline{\rho} \right\rangle \\ &\quad + q_j^{\mathrm{RANS}} + R_{ij}^{\mathrm{RANS}} \left\langle \overline{\rho}\tilde{u}_i \right\rangle / \left\langle \overline{\rho} \right\rangle + \frac{C_s'}{Pr'_T} \left(\overline{\Delta}^2 \overline{\rho} C_p \left|\tilde{S}\right| \frac{\partial \tilde{T}}{\partial x_j} - \left\langle \overline{\Delta}^2 \overline{\rho} C_p \left|\tilde{S}\right| \frac{\partial \tilde{T}}{\partial x_j} \right\rangle \right). \end{aligned} \tag{18}$$

Here, C_S' and Pr_T' are the constants in the compressible model. They verified the compressible CLES model in compressible turbulent channel flows, and the results are also very encouraging.

In principle, any RANS model, including algebraic model, SA model, *k*-ω model, *k*-ε model and SST model can be used to estimate the R_{ij}^{RANS} in Eqs. (16)–(18). To a certain extent, the results obtained from CLES depend on the accuracy of the estimation on R_{ij}^{RANS}. In turbulent channel flow, it was reported that the results obtained from CLES with algebraic model and SA model agreed extremely well with each other [38].

From Eq. (16), we can clearly see that the new model can generate small-scale fluctuations in the inner layer, which is typically deficient in the RANS region for hybrid RANS-LES methods. In their paper [38], Chen et al. validated CLES method by simulating incompressible turbulent channel flow at various Reynolds numbers and the flow past a circular cylinder at Re = 3 900 and 3×10^6.

Shown in Fig. 7a are the mean velocity profiles from LES with dynamics Smagorinsky model (LES-DSM), DES and CLES in incompressible turbulent channel flows at friction Reynolds number 2 000. The results are compared with the classical log-law profiles and the DNS results available. It is clearly seen that the mean velocity profile from CLES matches the DNS results and the log-law theory very well, while the mean profile of LES-DSM has an obvious shift-up and that of DES has the LLM defect.

CLES can also considerably reduce the prediction error of the skin-friction coefficient as shown in Fig. 7b, where the skin-friction coefficients from LES-DSM, DES and CLES are compared with the available DNS results and the Dean's estimations. It is clearly seen that the prediction error of CLES are much smaller than those from LES-DSM and DES.

Shown in Fig. 8 are the time-averaged pressure coefficients on the cylinder surface at (a) $Re = 3\,900$ and (b) $Re = 3\times10^6$. The CLES results are compared with those obtained from DES, coarse-grid DNS (CDNS, if available) and experimental measurements. The results show that the performance of CLES is comparable to, if not better than, that of DES at both Reynolds numbers for these turbulent flows with massive separations.

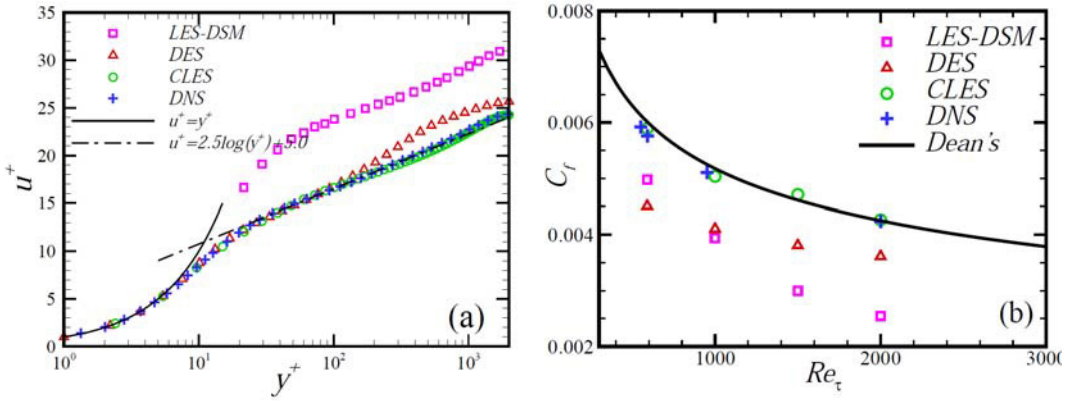

Fig. 7. (a) Mean velocity profiles from LES-DSM, DES and CLES at friction Reynolds number 2 000. The DNS results by Hoyas and Jiménez [41] is used as the reference. (b) The skin-friction coefficients predicted by LES-DSM, DES and CLES in terms of the friction Reynolds numbers. The available DNS calculated values and Dean's estimation [42] are also plotted for comparison.

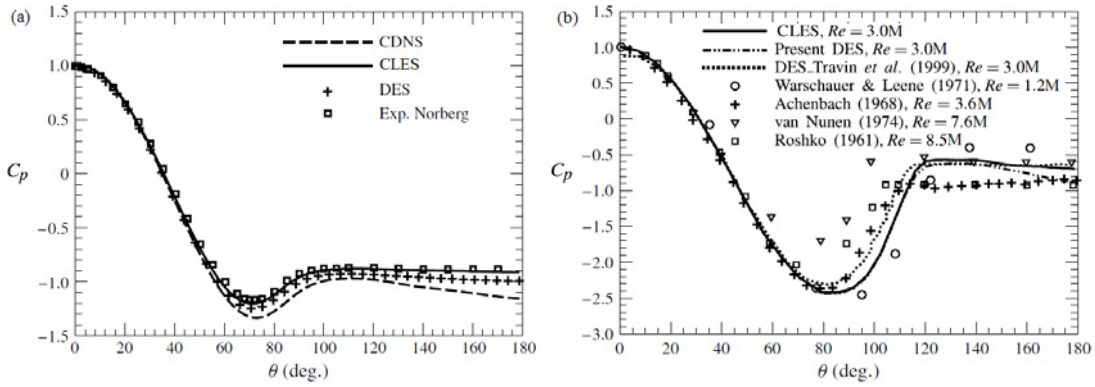

Fig. 8. Time-averaged pressure coefficient on the cylinder surface at (a) $Re = 3\,900$ and (b) $Re = 3\times10^6$. The front stagnation point is located at $\theta = 0^\circ$ [38].

Using the compressible CLES model, the students and collaborators in our group have simulated other flow problems, including transonic flow past a circular cylinder at Mach number 0.75 (see Fig. 9 left), flow past a deltawing with 50 degrees sweep-angle at 15 degrees angle of attack (see Fig. 9 right), flow past tandem cylinders (see Fig. 10 left) and flow past a commercial aircraft at 14 degrees angle of attack [43] (see Fig. 10 right).

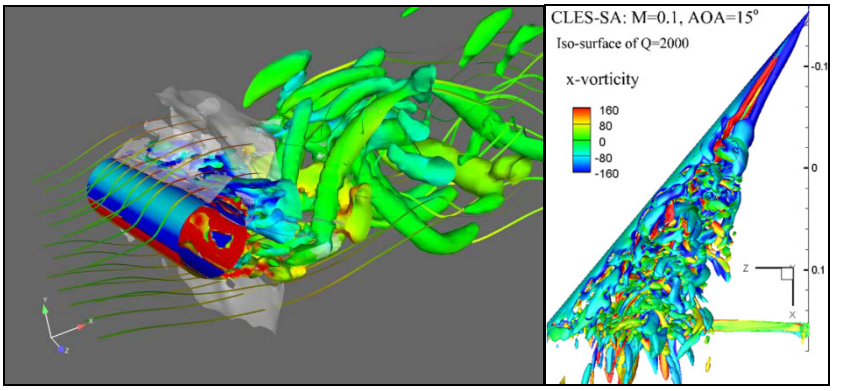

Fig. 9. Left: 3D shock waves, vortex structures and streamlines in flow past a circular cylinder at $M = 0.75$, $Re = 2\times10^5$; Right: vortex structures of flow past a deltawing with 50 degrees sweep-angle at 15 degrees angle of attack.

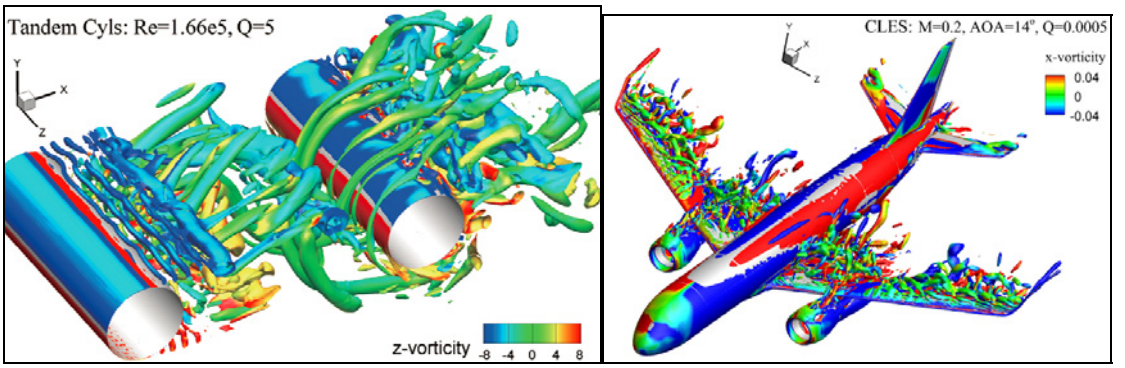

Fig. 10. Left: vortex structures of flow past tandem cylinders; Right: vortex structures of flow past a commercial aircraft at 14 degrees angle of attack.

4. Concluding remarks

Multiscale fluid phenomenon is ubiquitous in the nature. Multiscale modeling of fluid mechanics will play an important role in discovering new flow physics and modeling fluid engineering problems. Using physical constraints, we have developed new modeling methodologies, including hybrid molecular dynamics-continuum method for micro- and nanoscale fluid flows and constrained large eddy simulation for simulating realistic engineering turbulence. Our results demonstrate the capability of multiscale simulation methods for complex fluid systems and the necessity of physical constraints on the multiscale modeling.

Acknowledgements

This work is financially supported by the National Natural Science Foundation of China (10921202, 91130001, and 51176089) and the National Science and Technology Ministry under a sub-project of the "973" program (2009CB724101).

References

[1] Karniadakis GE, Beskok A, Aluru NR. *Microflows and Nanoflows: Fundamentals and Simulation.* Springer; 2005.
[2] Gad el Hak M. The fluid mechanics of microdevices–the freeman scholar lecture. *J Fluid Eng* 1999; **121**: 5–33.
[3] Bird GA. *Molecular gas dynamics and the direct simulation of gas flows*. Oxford: Clarendon Press; 1994.
[4] Wang M, Lan X, Li Z. Analysis of gas flows in micro- and nanochannels. *Int J Heat Mass Transfer* 2008; **51**: 3630–3641.
[5] Wang M, Li Z. An Enskog based Monte Carlo method for high Knudsen number non-ideal gas flows. *Computer Fluids* 2007; **36**: 1291–1297.
[6] Nie XB, Doolen GD, Chen SY. Lattice-Boltzmann simulations of fluid flows in MEMS. *J Statistical Physics* 2002; **107**: 279–289.
[7] Li ZH, Zhang HX. Gas-kinetic numerical studies of three-dimensional complex flows on spacecraft re-entry. *J Comput Phys* 2009; **228**: 1116–1138.
[8] Chen SZ, Xu K, Lee CB, Cai QD. A unified gas-kinetic scheme with moving mesh and velocity space adaptation. *J Comput Phys* 2012; **231**: 6643–6664.
[9] Chen SY, Doolen GD. Lattice Boltzmann method for fluid flows. *Annu Rev Fluid Mech* 1998; **30**: 329–364.
[10] http: //physics.wustl.edu/nd/event/qmcd09/Presentations/qmcd09Talks/orszag.pdf.
[11] Wang M, Wang J, Chen SY. Roughness and cavitations effects on electro-osmotic flows in rough microchannels using the lattice Poisson-Boltzmann methods. *J Comput Phys* 2007; **226**: 836–851.
[12] Wang M, Chen SY. Electroosmosis in homogeneously charged micro- and nanoscale random porous media. *J Colloids Interface Sci* 2007; **314**: 264–273.
[13] Wang M, Kang Q. Electrokinetic transport in microchannels with random roughness. *Analytical Chemistry* 2009; **81**: 2953–2961.
[14] Aidun CK, Clausen JR. Lattice-Boltzmann method for complex flows. *Annu Rev Fluid Mech* 2010; **42**: 439–472.
[15] Wei YK, Qian YH, Xu H. Lattice Boltzmann simulations of single bubble deformation and breakup in a shear flow. *The Journal of Computational Multiphase Flows* 2012; **4**: 111–118.
[16] Zhu LD, He GW, Wang SZ, Miller L, Zhang X, You Q, et al. An immersed boundary method based on the lattice Boltzmann approach in three dimensions, with application. *Computers & Mathematics with Applications* 2011; **61**: 3506–3518.
[17] Bisson M, Bernaschi M, Melchionna S, Succi S, Kaxiras E. Multiscale hemodynamics using GPU clusters. *Commun Comput Phys* 2012; **11**: 48–64.
[18] Nie XB, Chen SY, E WN, Robbins M. A continuum and molecular dynamics hybrid method for micro and Nano-Fluid Flow. *J Fluid Mech* 2004; **500**: 55–64.
[19] O'Connell ST, Thompson PA. Molecular dynamics-continuum hybrid computations: A tool for studying complex fluid flows. *Phys Rev E* 1995; **52**: 5792–5795.
[20] Hadjiconstantinou NG, Patera AT. Heterogeneous atomistic-continuum representations for dense fluid systems. *Intl J Mod Phys* 1997; **8**: 967–976.
[21] Liu J, Chen SY, Nie XB, Robbins M. A continuum-atomistic simulation of heat transfer in micro- and nano-flows. *J Comput Phys* 2007; **227**: 279–291.
[22] Nie XB, Robbins M, Chen SY. Resolving singular forces in cavity flow: Multiscale modeling from atomic to millimeter scales. *Phys Rev Lett* 2006; **96**: 134501.
[23] Liu J, Chen SY, Nie XB, Robbins M. A continnum-atomistic multi-Timescale algorithm for micro/nano flows. *Commun Comput Phys* 2008; **4**: 1279–1291.

[24] Behrens SH, Grier DG. The charge of glass and silica surface. *J Chem Phys* 2001; **115**: 6716–6721.
[25] Wang M, Revil A. Electrochemical charge of silica surface at high ionic strength in narrow channels. *J Collid Interface Sci* 2010; **343**: 381–386.
[26] Darden T, York D, Pedersen L. Particle mesh Ewald: an N.log(N) method for Ewald sums in large systems. *J Chem Phys* 1993; **98**: 10089–10092.
[27] Ogata S, Campbell TJ, Kalia RK, Nakano A, Vashishta P, Vemparala S. Scalable and portable implementation of the fast multipole method on parallel computers. *Comp Phys Commun* 2003; **153**: 445–461.
[28] Eastwood J, Hockney RW, Lawrence DN. P3M3DP: The three-dimensional periodic particle-particle/particle-mesh program. *Comp Phys Commun* 1980; **19**: 215–261.
[29] Liu J, Wang M, Chen SY, Robbins MO. Molecular simulations of eletrokinetic flows in rough nanochannels. *J Comput Phys* 2010; **229**: 7834–7847.
[30] Liu J, Wang M, Chen SY, Robbins MO. Uncovering molecular mechanisms of electrowetting and saturation with simulations. *Phys Rev Lett* 2012; **108**: 216101.
[31] Haase W, Braza M, Revell A, editors. *DESider-A European Effort on Hybrid RANS-LES Modelling: Results of the European-union funded project, 2004-2007*. Berlin: Springer; 2009.
[32] Spalart PR. Detached-eddy simulation. *Annu Rev Fluid Mech* 2009; **41**: 181–202.
[33] Fröhlich J, von Terzi D. Hybrid LES/RANS methods for the simulation of turbulent flows. *Prog Aerosp Sci* 2008; **44**: 349–377.
[34] Nikitin NV, Nicoud F, Wasistho B, Squires KD, Spalart PR. An approach to wall modelling in large-eddy simulations. *Phys Fluids* 2000; **12**: 1629–1632.
[35] Kraichnan KR. Decimated amplitude equations in turbulence dynamics. In: Dwoyer DL, Hussaini MY, Voigt RG, editors. *Theoretical Approaches to Turbulence*, Spinger; 1985; 91–135.
[36] Kraichnan KR, Chen SY. Is there a statistical mechanics of turbulence? *Physica D* 1989; **37**: 160–172.
[37] Shi YP, Xiao ZL, Chen SY. Constrained subgrid-scale stress model for large eddy simulation. *Phys Fluids* 2008; **20**: 011701.
[38] Chen SY, Xia ZH, Pei SY, Wang JC, Yang YT, Xiao ZL, Shi YP. Reynolds-stress-constrained large-eddy simulation of wall-bounded turbulent flows. *J Fluid Mech* 2012; **703**: 1–28.
[39] Pope SB. *Turbulent Flows*. 1st ed. Cambridge University Press; 2000.
[40] Jiang Z et al. Constrained large eddy simulation in compressible turbulent channel flow. submitted to *Phys Fluids*.
[41] Hoyas S, Jiménez J. Scaling of velocity fluctuations in turbulent channels up to $Re_\tau = 2003$. *Phys Fluids* 2006; **18**: 011702.
[42] Dean RB. Reynolds number dependence of skin friction and other bulk flow variables in two-dimensional rectangular duct flow. *Trans ASME: J Fluid Engng* 1978; **100**: 215–223.
[43] Chen SY, Chen YC, Xia ZH, Qu K, Shi YP, Xiao ZL, et al. Constrained large-eddy simulation and detached eddy simulation of flow past a commercial aircraft at 14 degrees angle of attack. *Sci China-Phys Mech Astron* 2013; **56**: 270–276.